Abstract: We characterize the saturable absorption of the second (E_{22}) electronic transition of a sample of single-walled carbon nanotubes and use it to mode-locked an Ytterbium fiber ring laser. The modulation depth of $\sim$ 15% was found to be similar to the corresponding E_{11} transition ($\sim$ 13%), but the saturation intensity ($\sim$ 220 MW cm^{-2}) about an order of magnitude larger ($\sim$ 10 MW cm^{-2}). We achieved a 15 MHz mode-locked pulse train with an output pulse duration of 6.5 ps. For comparison we also demonstrate stable mode-locking on the E_{11} transition, of the same nanotubes, with an Erbium fiber ring laser, producing 1.1 ps pulses. Using the E_{22} transition should enable the use of carbon nanotube saturable absorbers at shorter wavelengths than currently possible with the E_{11} transition, which are limited by the smallest achievable nanotube dimensions.

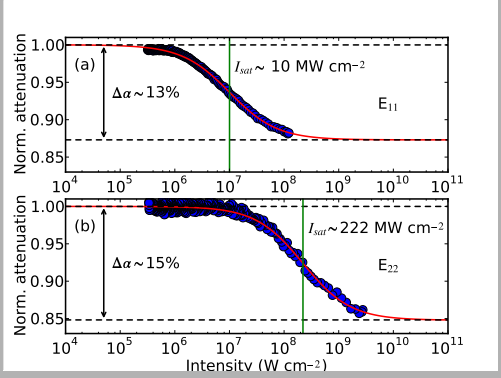

Saturable absorption measurements of single-walled carbon nanotubes by the Z-scan method. (a) E_{11} and (b) E_{22} transition.

Using the E_{22} transition of carbon nanotubes for fiber laser mode-locking

J. C. Travers, [1,*] *J. Morgenweg,* [2] *E. D. Obraztsova,* [3] *A. S. Lobach,* [4] *A. I. Chernov,* [3] *E. J. R. Kelleher,* [1] *S. V. Popov,* [1] *and J. R. Taylor* [1]

[1] Femtosecond Optics Group, Physics Department, Prince Consort Road, Imperial College, London SW7 2AZ, UK
[2] Jonas new home
[3] A.M. Prokhorov General Physics Institute, 38 Vavilov Street, 119991, Moscow, Russia
[4] Institute of Problems of Chem. Physics, RAS, 142432, Chernogolovka, Moscow Region, Russia

Received: September 16, 2010
Published online: September 16, 2010

Key words: Mode-locked lasers; Lasers, fiber; Nanomaterials

1. Introduction

The use of single-walled carbon nanotubes (SWNTs) as saturable absorbers for initiating and maintaining mode-locking has created wide interest [1–9], and fiber lasers utilizing SWNTs have been demonstrated at a range of operating wavelengths [9–18]. This interest arises from the key properties of SWNTs for mode-locking lasers [10, 6]: sub-picosecond characteristic transition times; a high damage threshold; environmental stability; all-fiber integration. Combined, these properties make SWNTs competitive with conventional fiber mode-locking techniques such as nonlinear polarization evolution [19], or semiconductor saturable absorbers (SESAMs) [20].

The great majority of mode-locked lasers demonstrated use the fundamental (E_{11}) transition of semiconducting nanotubes, which corresponds to the single real gap in the electron density of states [21]. In contrast, only a few groups have reported saturable absorption and mode-locking of bulk lasers, using the second transition (E_{22}) [22, 23], corresponding to a pseudo-gap [21]. We recently expressly demonstrated that this transition can also be used to mode-lock fiber lasers [24], where the mode-locking dynamics differ from solid-state lasers. It is of fundamental interest that a second electronic transition can be used for saturable absorption as it significantly increases the absorption energy for a given nanotube diameter [10], and opens the possibility of mode-locking shorter wavelength systems, below 1 μm, towards the visible spec-

* Corresponding author: e-mail: john.travers03@imperial.ac.uk

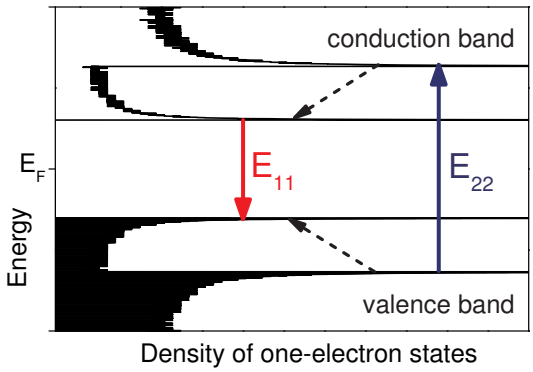

Figure 1 Schematic of the levels involved in saturable absorption of E_{22}. E_F=Fermi level.

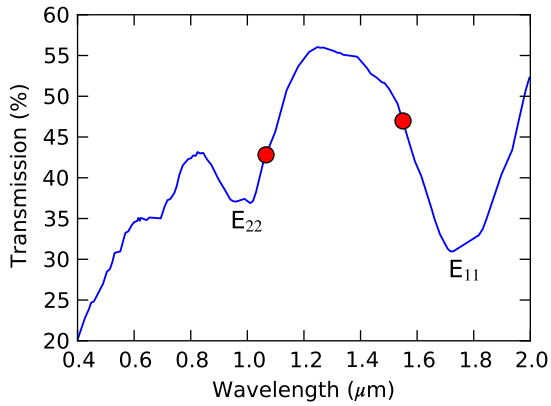

Figure 2 Linear transmission spectrum of the carbon nanotube film used in the saturable absorption and mode-locking experiments. The wavelengths at which the saturable absorption was measured, and mode-locking was achieved are shown by the red circles. The E_{11} and E_{22} transition absorptions are also indicated.

tral region, something that is hard to achieve on the E_{11} transition with currently realizable nanotube dimensions (0.3 nm [25]). Also the shorter E_{22} lifetime [26], may affect mode-locking behaviour.

Figure 1 illustrates the mechanism to obtain saturable absorption on the E_{22} transition. After excitation, the electron must pass to the lower energy transition, corresponding to the real gap E_{11}. This has been illustrated by photoluminescence (PL) measurements, where the signals have been observed only for E_{11} transitions of different nanotubes [21]. Nevertheless other optical experiments (for instance, resonant Raman scattering in SWNTs) have shown that the pseudo-gaps could also demonstrate resonant phenomena.

To further understand this potential, in this work, we report on detailed comparative measurements of the saturable absorption properties of both the E_{11} and E_{22} transitions in the same sample of highly-purified nanotubes, and realize a mode-locked Ytterbium fiber laser operating at a wavelength of 1.06 μm. We also demonstrate an Erbium fiber laser mode-locked on the E_{11} transition of the same set of nanotubes.

2. Nanotube sample

A transparent carboxymetylcellulose film with homogeneously dispersed individual SWNTs[27], was used as a saturable absorber. The same film already has been used in Er- and Tm- fiber lasers [9, 15]. In the Er case, a minimal pulse duration of 177 fs was achieved [9]. In the Tm case, the longest wavelength of operation was 1.9 μm [15]. The transmittance spectrum of this film is shown in Fig. 2. The clean two peaked spectrum is an indication of the purity of the nanotubes in the film, as the width of the absorption bands is related to the diameter distribution of the nanotubes. The absorption centered at 1.75 μm is due to the E_{11} transition, and was sufficiently broad to allow mode-locking at 1.55 μm. The peak around 1.0 μm is due to the

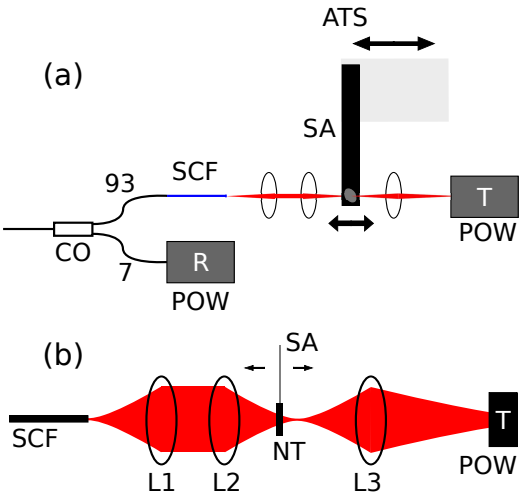

Figure 3 (a) Overview of the Z-scan setup. (b) Close up of the Z-scan optics. CO - coupler, POW - power meter, SCF - small core fibre, SA - scanning arm, ATS - automated translation stage, R - reference, T - transmitted, L1 and L2 - focussing lenses, L3 - collection lens, NT - nanotube sample.

E_{22} transition [28], even when taking into account excitonic effects [29].

3. Z-scan measurements

3.1. Experimental setup

The Z-scan setup is shown in Fig. 3. The pump light is pased through a fused fiber coupler to split 7% of the

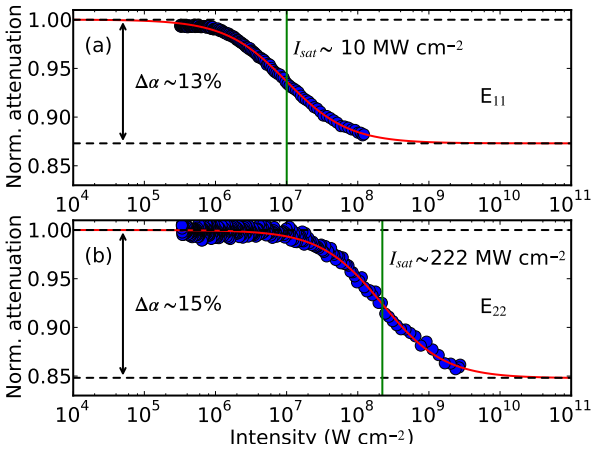

Figure 4 Saturable absorption measurements by the Z-scan method. (a) E_{11} and (b) E_{22} transitions.

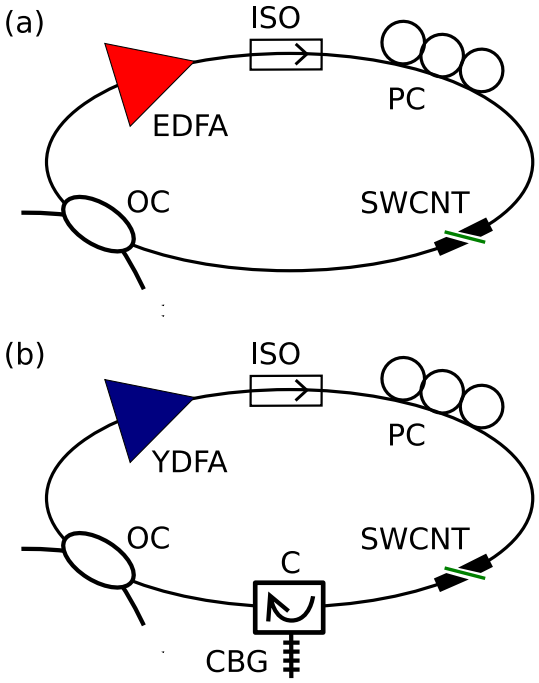

Figure 5 Experimental setup of the mode-locked ring lasers. (a) The Erbium based E_{11} transition laser. (b) The Ytterbium based E_{22} transition laser. EDFA - erbium doped fibre amplifier, YDFA - ytterbium doped fibre amplifier, SWNT - single-walled carbon nanotube saturable absorber, PC - polarization controller, OC - fused fiber output coupler, ISO - isolator, C - circulator, CBG - chirped Bragg grating.

power to a reference power meter. The remaining power is then coupled into a small core, high NA fibre (Nufern UHNA 3), the output of which is imaged by a pair of identical aspheric lenses. An automated translation stage moves the sample arm and nanotube film through the focus. A third lens collects the light transmitted through the sample to a second power meter. To pump the E_{11} transition we used an amplified mode-locked Erbium fiber laser with a repetition rate of 14 MHz and pulse duration of 3 ps. For the E_{22} transition we used a mode-locked Ytterbium fiber laser followed by an amplifier and grating compressor system to produce 0.9 ps pulses at a repetition rate of 47.5 MHz. The resulting peak intensities at the Z-scan focus were approximately 125 MW cm^2 and 2.6 GW cm^2 for the E_{11} and E_{22} transitions respectively.

3.2. Results and discussion

The results of the Z-scan measurements are shown in Fig. 4. It should be noted that there is some uncertainty as to the accuracy of the intensity scale due uncertainity in the exact pump pulse shape. The red fit curve is based on the instantaneous saturable absorption model:

$$\alpha(t) = \frac{\Delta\alpha}{1 + \frac{I(t)}{I_{sat}}} + (1 - \Delta\alpha). \qquad (1)$$

Due to the fact that for both the E_{11} and E_{22} transition the pump pulses are significantly longer than the transition lifetimes, by a factor of ~ 8 and ~ 23 respectively [26], the instantaneous model ought to reasonable. The normalised modulation depths ($\Delta\alpha$) of 13% and 15% respectively for the E_{11} and E_{22} transitions are very similar, however, the saturation intensities (I_{sat}) of ~ 10 MW cm^{-2} and ~ 220 MW cm^{-2} are different by an order of magnitude. This difference is expected, and can almost entirely be accounted for, from the respective transition lifetimes of ~ 400 fs and ~ 40 fs [26].

The E_{22} modulation depth ought to be sufficient to modelock a fiber laser, and the increased saturation intensity, although larger than the E_{11} transition of nanotubes, and also of that of semiconductor staurable absrober mirrors (SESAMs), is still significantly smaller than required in nonlinear polarisation rotation systems, ansd should not present a problem for fibre lasers.

4. Mode-locking results

4.1. Experimental setup

We constructed an Erbium and Ytterbium fibre ring laser to test modelocking on both the E_{11} and E_{22} transitions. The experimental setups for the lasers are shown in Fig. 5. Both lasers were constructed from isotropic single-mode fiber. The polarization controllers were included to check the output pulse dependence on polarization state. The carbon nanotube films were sandwiched between two FC-APC connectors. In the Ytterbium ring laser a fiber integrated circulator and chirped Bragg grating with a dispersion of 35.7 ps/nm was included to compensate for

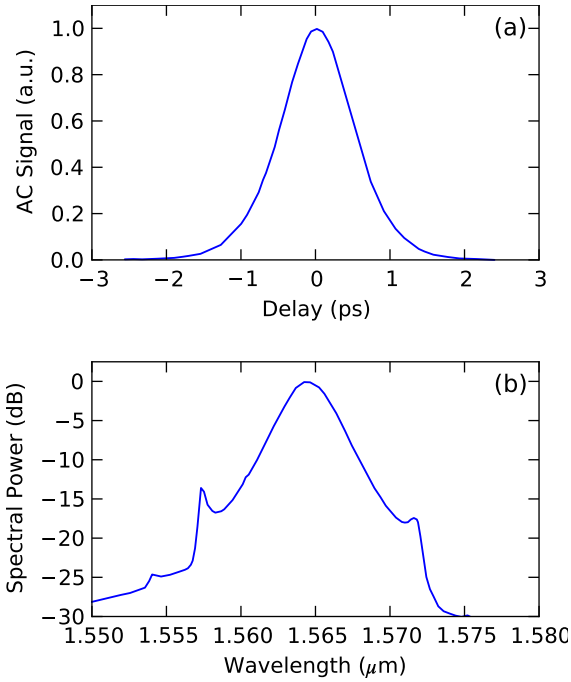

Figure 6 Autocorrelation (a) and optical spectrum (b) of the Erbium ring laser operating on the E_{11} transition.

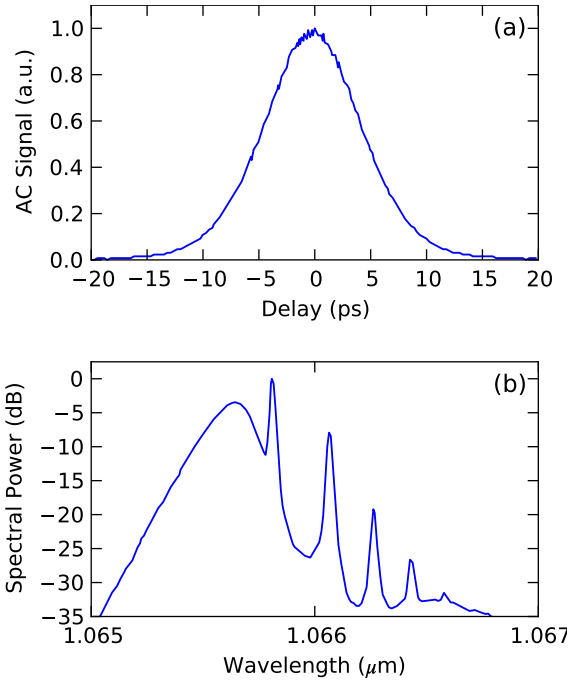

Figure 7 Autocorrelation (a) and optical spectrum (b) of the Ytterbium ring laser operating on the E_{22} transition.

the normal dispersion of the other cavity components; due to this extremely high value the overall cavity dispersion was strongly anomalous. The Erbium system was naturally anomalously dispersive and no compensation was required to operate in the soliton regime. The output coupler was 50% for the Erbium laser and 15% for the Ytterbium laser. In both setups exactly the same nanotube film was used.

4.2. Results and discussion

Both laser setups were self-starting upon reaching threshold, and mode-locking was maintained through approximately 10% tuning of the pump power. For increasing powers Q-switching was observed. The pulse trains exhibited no transient dynamics and remained stable with a single pulse per cavity round-trip. The polarization control had little effect on the pulse train and output characteristics.

Figure 6 shows the results obtained with the Erbium ring laser. The full width at half maximum (FWHM) of the second-harmonic intensity autocorrelator signal was 1.1 ps, which corresponds to 0.7 ps if we assume a sech^2 pulse shape. [WHAT ABOUT CHIRP!]. No attempt was made to correctly tune the cavity dispersion and nonlinearity for short pulse operation, although that can lead to considerably shorter pulses [9]. The central wavelength of the pulse was 1.565 μm and the spectral width 3.12 nm. From inspection of Fig. 2 it is clear that this laser was mode-locked using the short wavelength edge of the E_{11} transition of the nanotubes.

Figure 7 shows the results obtained with the Ytterbium ring laser. For this system the FWHM autocorrelation duration was 10.0 ps, which corresponds to 6.5 ps assuming a sech^2 pulse shape. Again, no attempt was made to fully dispersion compensate the cavity, rather the chirped Bragg grating ensured we were operating in the strongly anomalous regime. Full cavity dispersion compensation with bulk gratings or photonic band-gap fiber should lead to shorter pulse operation [12, 14]. The central laser wavelength was 1.066 μm and the spectral bandwidth was 0.18 nm. This corresponds to a time-bandwidth product of 0.31 indicating that the output pulses were not strongly chirped. The average output power was 170 μW. The repetition rate of the laser was 15.2 MHz.

While the wavelength of the Erbium laser clearly indicates it is operating on the E_{11} transition (see Fig. 2), the Ytterbium laser wavelength is too short for his transition and must be operating on the second absorption peak of the nanotubes, i.e. the E_{22} transition. Despite this the laser exhibited similar qualitative behavior as the Erbium system operating on the E_{11} transition.

5. Conclusions

The ability to saturate the fast E_{22} transition raises a number of possibilities. Firstly, the larger transition energy of

the E_{22} level means that mode-locking at shorter wavelengths is viable, potentially into the visible spectral region. Secondly, because the electron falls to the E_{11} level after E_{22} excitation, the E_{11} saturable absorption could be controllable via the E_{22} transition. Finally, it may be possible to simultaneously mode-lock both transitions in a dual wavelength fiber laser.

In conclusion we have characterized the saturable absorption properties of the E_{11} and E_{22} transitions of a high-purity film of single-wall carbon nanotubes. We found that the modulation depths were similar but the saturation intensity was one order of magnitude smaller for the E_{11} compared to the E_{22} transition. This is accounted for by the similar disparity in transition lifetimes. Mode-locking of a fiber laser was achieved on both transitions.

6. Acknowledgements

JCT is an Imperial College Junior Research Fellow, EJRK is supported by an EPSRC studentship, SVP is a Royal Society Industry Fellow and JRT is a Royal Society Wolfson Research Merit Award holder. The GPI RAS team is supported by RFBR-07-02-91033 project and RAS Research program “Femtosecond Optics”.

References

[1] Y. Chen, N. Raravikar, L. Schadler, P. Ajayan, Y. Zhao, T. Lu, G. Wang, and X. Zhang, Appl. Phys. Lett. 81, 975 (2002).
[2] Y. Sakakibara, S. Tatsuura, H. Kataura, M. Tokumoto, and Y. Achiba, JAPANESE JOURNAL OF APPLIED PHYSICS PART 2 LETTERS 42, 494–496 (2003).
[3] S. Set, H. Yaguchi, Y. Tanaka, M. Jablonski, Y. Sakakibara, A. Rozhin, M. Tokumoto, H. Kataura, Y. Achiba, and K. Kikuchi, in *Optical Fiber Communications Conference, 2003. OFC 2003*, pages PD44–P1–3 vol.3 (2003), doi: {10.1109/OFC.2003.1248625}.
[4] N. Il’ichev, E. Obraztsova, S. Garnov, and S. Mosaleva, Quantum Electron. 34, 572–574 (2004).
[5] N. Il’ichev, E. Obraztsova, P. Pashinin, V. Konov, and S. Garnov, Quantum Electron. 34, 785–786 (2004).
[6] S. Yamashita, Y. Inoue, S. Maruyama, Y. Murakami, H. Yaguchi, M. Jablonski, and S. Y. Set, Opt. Lett. 29, 1581–1583 (2004).
[7] T. Schibli, K. Minoshima, H. Kataura, E. Itoga, N. Minami, S. Kazaoui, K. Miyashita, M. Tokumoto, and Y. Sakakibara, Opt. Express 13, 8025–8031 (2005).
[8] A. Rozhin, V. Scardaci, F. Wang, F. Hennrich, I. White, W. Milne, and A. Ferrari, physica status solidi (b) 243, 3551–3555 (2006).
[9] A. V. Tausenev, E. D. Obraztsova, A. S. Lobach, A. I. Chernov, V. I. Konov, P. G. Kryukov, A. V. Konyashchenko, and E. M. Dianov, Applied Physics Letters 92, 171113 (2008), doi:10.1063/1.2918450.
[10] S. Set, H. Yaguchi, Y. Tanaka, and M. Jablonski, Selected Topics in Quantum Electronics, IEEE Journal of 10, 137–146 (2004).
[11] Y. Song, S. Set, S. Yamashita, C. Goh, and T. Kotake, IEEE PHOTONICS TECHNOLOGY LETTERS 17, 1623 (2005).
[12] C. Goh, K. Kikuchi, S. Set, D. Tanaka, T. Kotake, M. Jablonski, S. Yamashita, and T. Kobayashi, Lasers and Electro-Optics, 2005.(CLEO). Conference on 3 (2005).
[13] A. Rozhin, Y. Sakakibara, S. Namiki, M. Tokumoto, H. Kataura, and Y. Achiba, Appl. Phys. Lett. 88, 051118 (2006).
[14] J. W. Nicholson, R. S. Windeler, and D. J. DiGiovanni, Opt. Express 15, 9176–9183 (2007).
[15] M. Solodyankin, E. Obraztsova, A. Lobach, A. Chernov, A. Tausenev, V. Konov, and E. Dianov, Opt. Lett. 33, 1336–1338 (2008).
[16] K. Kieu and F. W. Wise, Opt. Express 16, 11453–11458 (2008).
[17] F. Wang, A. G. Rozhin, Z. Sun, V. Scardaci, I. H. White, and A. C. Ferrari, Phys. Status Solidi B 245, 2319–2322 (2008).
[18] S. Kivistö, T. Hakulinen, A. Kaskela, B. Aitchison, D. P. Brown, A. G. Nasibulin, E. I. Kauppinen, A. Härkönen, and O. G. Okhotnikov, Opt. Express 17, 2358–2363 (2009).
[19] V. Matsas, T. Newson, D. Richardson, and D. Payne, Electronics Letters 28, 1391–1393 (1992).
[20] E. De Souza, C. Soccolich, W. Pleibel, R. Stolen, J. Simpson, and D. DiGiovanni, Electronics Letters 29, 447–449 (1993).
[21] S. Bachilo, M. Strano, C. Kittrell, R. Hauge, R. Smalley, and R. Weisman, Science 298, 2361–2366 (2002).
[22] J. Yim, W. Cho, S. Lee, Y. Ahn, K. Kim, H. Lim, G. Steinmeyer, V. Petrov, U. Griebner, and F. Rotermund, Appl. Phys. Lett. 93, 161106 (2008).
[23] A. Schmidt, S. Rivier, G. Steinmeyer, J. Yim, W. Cho, S. Lee, F. Rotermund, M. Pujol, X. Mateos, M. Aguiló, et al., Opt. Lett. 33, 729–731 (2008).
[24] J. C. Travers, E. D. Obraztsova, A. S. Lobach, A. I. Chernov, E. J. R. Kelleher, S. V. Popov, and J. R. Taylor, in *CLEO/Europe and EQEC 2009 Conference Digest*, page CJ10, Optical Society of America (2009).
[25] J. P. Zhai, W. W. Peng, I. L. Li, S. C. Ruan, and Z. K. Tang, J. Phys. Chem. C 112, 11702–11706 (2008), doi:10.1021/jp802218x.
[26] C. Manzoni, A. Gambetta, E. Menna, M. Meneghetti, G. Lanzani, and G. Cerullo, Phys. Rev. Lett. 94, 207401 (2005).
[27] A. I. Chernov, E. D. Obraztsova, and A. S. Lobach, PHYSICA STATUS SOLIDI B-BASIC SOLID STATE PHYSICS 244, 4231–4235 (2007).
[28] H. Kataura, Y. Kumazawa, Y. Maniwa, I. Umezu, S. Suzuki, Y. Ohtsuka, and Y. Achiba, Synthetic Metals 103, 2555–2558 (1999).
[29] R. Weisman and S. Bachilo, Nano Letters 3, 1235–1238 (2003).